Thermal Property Simulation of ZrO_2-based Nanocomposites for Inert Matrix Fuel

Vivek Raj [a], Qusai M. Mistarihi [b], Ho Jin Ryu [b*]
[a]*Indian Institute of Technology-Kanpur, Kalyanpur, Kanpur, Uttar Pradesh 208016, India*
[b]*Dept. of Nuclear and Quantum Engineering, KAIST, 291 Daehakro, Yuseong, Daejeon 305-701, Republic of Korea*
[*]*Corresponding author: hojinryu@kaist.ac.kr*

1. Introduction

Burning excess Pu and Minor Actinides (MA) in light water reactors or fast reactors might be an alternative option for managing transuranic elements (TRU) with very long half-lives. Inert matrix fuel (IMF) is a promising concept to incinerate TRU without further producing plutonium from U-238 which is a main host material for current nuclear fuels containing fissile isotopes such as U-235 or Pu-239. ZrO_2 is one of the suitable materials for a matrix of IMF because it has an excellent chemical stability and an irradiation resistance [1]. However, ZrO_2 has a very low thermal conductivity around 3 W/mK at 1000^{o}C which is not beneficial for the in-reactor fuel performances, and the low thermal conductivity might result in a high fission gas release and high fuel swelling [2]. Therefore, enhancing the thermal conductivity of ZrO_2 might be very effective in improving the fuel performance of ZrO_2 based IMF. Metallic wires with a high thermal conductivity can be used as reinforcement for ZrO_2. In this study, Mo wire has been selected for the modeling and characterization of ZrO_2-based nanocomposites because Mo has a high thermal conductivity approximately 138 W/mK and a relatively low neutron absorption cross section. The effect of interfacial resistance between ZrO_2 and Mo wire has also been studied for some reinforcement arrays.

2. Experimental Procedure and Finite Element Simulation

2.1 Experimental Fabrication

Mo-reinforced ZrO_2 composite pellets were fabricated by spark plasma sintering of mixed powder of Mo and ZrO_2 powder at 1700^{o}C under vacuum. Mo wire, mesh, and powder were used to investigate the effects of interconnection of thermal conductive reinforcements. The thermal conductivities of the fabricated pellets were measured by the laser flash method and then compared with computational simulation results using the finite element method.

2.2 Finite Element Modelling

In this study, two types of reinforcement have been used one is three-dimensional interconnected and other is particulate reinforcement shown in Fig. 1 and 2. And three dimensional interconnected reinforcement cases have been analyzed for isotropic and anisotropic thermal conductivity. The composite structures are created by repeating idealized particle or three-dimensional network unit cells [3].

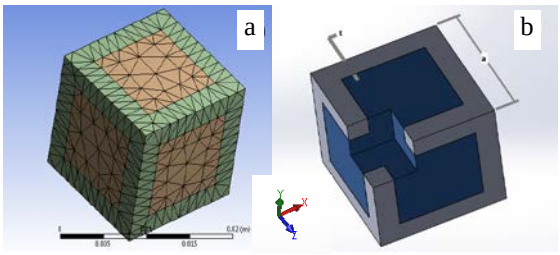

Fig. 1. 3-D interconnected reinforcement; (a) mesh used for finite element analysis and (b) schematic unit cell of simplified three-dimensional continuous microstructure.

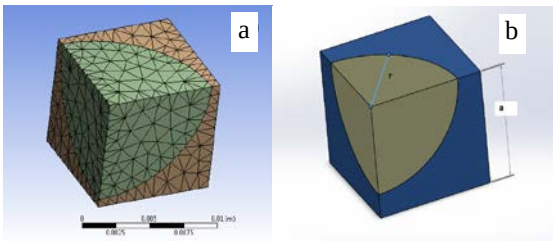

Fig. 2. Particle reinforcement; (a) mesh used for finite element analysis and (b) one eighth unit cell used for simplified three-dimensional continuous microstructure.

2.2.1 Isotropic cases

A Cartesian coordinate system (x, y, z) was employed in the simulation for implementing boundary conditions. For a particle-reinforced composite, the unit cell analyzed numerically is in the domain defined by $0 \le x \le a/2$, $0 \le y \le a/2$, and $0 \le z \le a/2$ (Fig. 2). The unit cell for the three dimensional network-reinforced composites is defined by $0 \le x \le a$, $0 \le y \le a$, and $0 \le x \le a$ (Fig. 1). In the simulation, the volume fraction of reinforcement was kept 5% and the values of constant temperature are changed to understand its influence on the thermal properties of composites. Boundary conditions used are as follows:

- Heat Flux= Q_1 @ y= 0
- T= Constant @ y= a (for 3-D interconnected)
- T= Constant @ y= a/2 (for particle)

- Q=0 @ z= 0 & a (for 3-D interconnected)

- Q=0 @ z= a/2 (for particle)
- Q=0 @ x= 0 & a (for 3-D interconnected)
- Q=0 @ x= a/2 (for particle)

2.2.2 Anisotropic cases

To study the effect of anisotropy in thermal properties of composites, a mesh model of Mo has been introduced in ZrO_2 cube model (51x35.8x51) and heat flux is applied in two different directions as shown in Fig 3&4. The Boundary conditions for the two models are as follows:

a) Heat flux parallel to mesh plane
- Q=0 @ y= 0 & 51
- Q=0 @ z= 0 & 35.8
- Q= 10^3 W/m^2 @ x= 51 (right face)
- T= Constant @ x= 0 (left face)

b) Heat flux perpendicular to mesh plane
- Q=0 @ y= 0 & 51
- Q=0 @ x= 0 & 51
- Q= 10^3 W/m^2 @ z= 0 (back face)
- T= Constant @ z= 35.8 (front face)

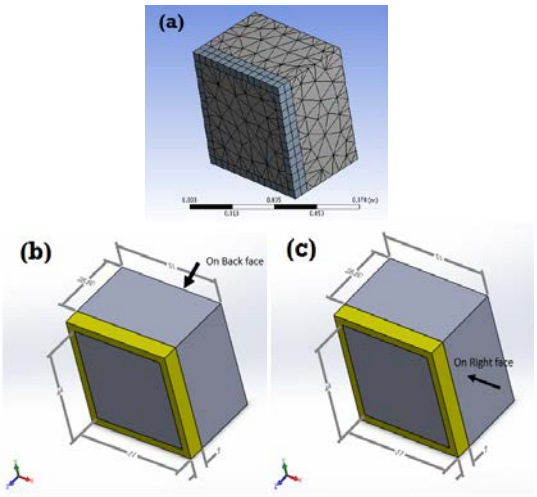

Fig 3. a) Mesh used for finite element analysis b) model used to apply heat flux perpendicular to mesh plane c) model used to apply heat flux parallel to mesh plane.

The finite element method is used to study the thermal properties with boundary conditions as discussed above for different cases. The effective or macroscopic average thermal conductivities of the composites can then be calculated using the fundamental conductivity equation. Finite element simulation is conducted using ANSYS^{TM} (licensed to IIT-Kanpur) and the thermal solid element used for 3D interconnected reinforcement is SOLID 70 and for particle reinforcement is SOLID 87.

3. Results

Thermal conductivity of the MMCs has been measured at different temperatures and graph to show the variation has been plotted as shown in Fig. 4,5,6 and 7 and user defined function (UDF) of ANSYS are used to determine the average temperature of face where temperature distribution is not uniform. To understand the effect of interfacial resistance, the anisotropic model is simulated for different values of contact resistance between matrix and reinforcement and also the dimension of unit cells are changed to understand the effect of dimensions as shown in the data below.

Table 1. The variation of composite thermal conductivities with interfacial resistance for heat flux perpendicular to mesh plane

Dimension (μm)	Thermal conductivity (W/mK)	Resistance $(W/m^2K)^{-1}$
51*51*35.8	6.92E+00	1E-1
51*51*35.8	6.92E+00	1E-2
51*51*35.8	6.92E+00	1E-3
51*51*35.8	6.93E+00	1E-4
51*51*35.8	7.04E+00	1E-5
51*51*35.8	7.63E+00	1E-6
51*51*35.8	8.33E+00	1E-7
51*51*35.8	8.49E+00	1E-8
51*51*35.8	8.51E+00	1E-9
51*51*35.8	8.52E+00	1E-10

Dimension (μm)	Thermal conductivity (W/mK)	Resistance $(W/m^2K)^{-1}$
510*510*358	6.92E+00	1
510*510*358	6.92E+00	1E-1
510*510*358	6.92E+00	1E-2
510*510*358	6.93E+00	1E-3
510*510*358	7.04E+00	1E-4
510*510*358	7.63E+00	1E-5
510*510*358	8.33E+00	1E-6
510*510*358	8.49E+00	1E-7
510*510*358	8.51E+00	1E-8
510*510*358	8.52E+00	1E-9

Dimension (μm)	Thermal conductivity (W/mK)	Resistance $(W/m^2K)^{-1}$
5100*5100*3580	6.92E+00	1
5100*5100*3580	6.92E+00	1E-1
5100*5100*3580	6.93E+00	1E-2
5100*5100*3580	7.04E+00	1E-3
5100*5100*3580	7.63E+00	1E-4
5100*5100*3580	8.33E+00	1E-5
5100*5100*3580	8.49E+00	1E-6
5100*5100*3580	8.51E+00	1E-7
5100*5100*3580	8.51E+00	1E-8
5100*5100*3580	8.52E+00	1E-9

Table 2. The variation of composite thermal conductivities with interfacial resistance for heat flux perpendicular to mesh plane

Dimension (μm)	Thermal conductivity (W/mK)	Resistance $(W/m^2K)^{-1}$
51*51*35.8	9.53E+00	1E-2
51*51*35.8	9.53E+00	1E-3
51*51*35.8	9.58E+00	1E-4
51*51*35.8	9.82E+00	1E-5
51*51*35.8	1.02E+00	1E-6
51*51*35.8	1.05E+00	1E-7
51*51*35.8	1.06E+00	1E-8
51*51*35.8	1.06E+00	1E-9
51*51*35.8	1.07E+00	1E-10
51*51*35.8	1.08E+00	1E-11

Dimension (μm)	Thermal conductivity (W/mK)	Resistance $(W/m^2K)^{-1}$
510*510*358	9.53E+00	1
510*510*358	9.53E+00	1E-1
510*510*358	9.53E+00	1E-2
510*510*358	9.58E+00	1E-3
510*510*358	9.82E+00	1E-4
510*510*358	1.02E+00	1E-5
510*510*358	1.05E+00	1E-6
510*510*358	1.06E+00	1E-7
510*510*358	1.06E+00	1E-8
510*510*358	1.07E+00	1E-9

Dimension (μm)	Thermal conductivity (W/mK)	Resistance $(W/m^2K)^{-1}$
5100*5100*3580	9.53E+00	1
5100*5100*3580	9.53E+00	1E-1
5100*5100*3580	9.58E+00	1E-2
5100*5100*3580	9.83E+00	1E-3
5100*5100*3580	1.02E+00	1E-4
5100*5100*3580	1.05E+00	1E-5
5100*5100*3580	1.06E+00	1E-6
5100*5100*3580	1.06E+00	1E-7
5100*5100*3580	1.07E+00	1E-8
5100*5100*3580	1.08E+00	1E-9

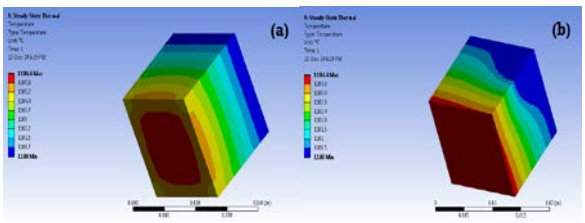

Fig. 4. Temperature profile of ZrO_2-Mo model; a) 3D interconnected reinforced, b) Particle reinforced

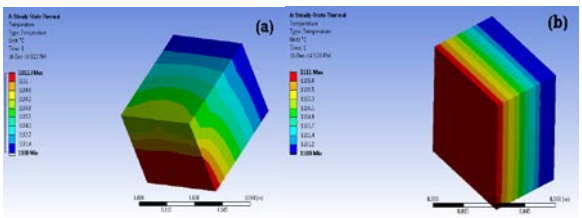

Fig. 5. Temperature profile of ZrO_2-Mo model; a) heat flux parallel to mesh plane, b) heat flux perpendicular to mesh plane

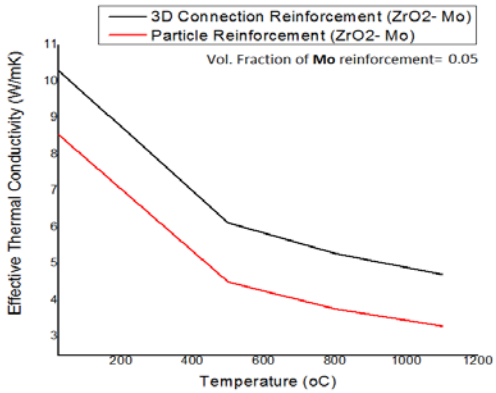

Fig. 6. Plot between Thermal Conductivity and temperature for 3D interconnected and particle reinforcement.

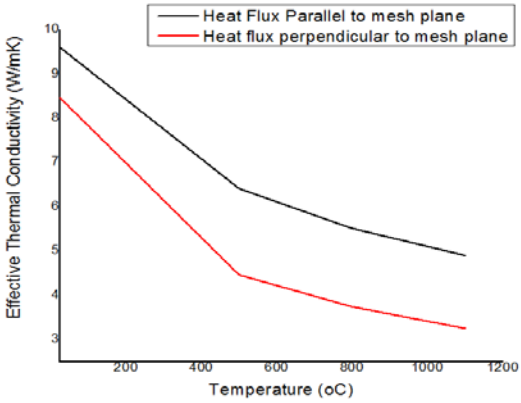

Fig. 7. Plot for anisotropic case of ZrO_2-Mo model in which heat flux is applied parallel and perpendicular to mesh plane.

4. Conclusions

The experimental results and computational simulations presented a good agreement in estimating the effects of the reinforcement on the thermal conductivities of Mo reinforced ZrO_2 nanocomposites. It is found that one of the most contributing factors to the enhancement of the thermal conductivity of ZrO_2-based nanocomposites is the interconnection of Mo wire.

REFERENCES

[1] C.Degueldre, T.Arima, Y.W.Lee, Thermal conductivity of zirconia based inert matrix fuel: use and abuse of the formal models for testing new experimental data. Journal of nuclear materials, Vol.319, p.6, 2003.
[2] S.Yeo, E.Mckenna, R.Baney, G.Subhash, J.Tulenko, Enhanced thermal conductivity of uranium dioxide–silicon carbide composite fuel pellets prepared by Spark Plasma Sintering (SPS). Journal of Nuclear Materials, Vol.433, p.66, 2013.
[3] X.D. Liu, J.S. Zhang, X.M. Cao, H. Zhang, Finite element simulation of the thermal properties of particulate and continuous network-reinforced, Proceedings of the Institution of Mechanical Engineers, Part B: Journal of Engineering Manufacture, Vol.219, p.111, 2005.